Proteins identified through predictive metagenomics as potential biomarkers for the detection of microbiologically influenced corrosion

Giovanni Pilloni (iD), Fang Cao, Megan Ruhmel, Pooja Mishra

Corporate Strategic Research, ExxonMobil Research and Engineering Company, Annandale, NJ 08801, USA
Correspondence should be addressed to: Giovanni Pilloni. E-mail: giovanni.pilloni@exxonmobil.com

Abstract: The unpredictability of microbial growth and subsequent localized corrosion of steel can cause significant cost for the oil and gas industry, due to production downtime, repair, and replacement. Despite a long tradition of academic research and industrial experience, microbial corrosion is not yet fully understood and thus not effectively controlled. In particular, biomarkers suitable for diagnosing microbial corrosion which abstain from the detection of the classic signatures of sulfate-reducing bacteria are urgently required. In this study, a natural microbial community was enriched anaerobically with carbon steel coupons and in the presence of a variety of physical and chemical conditions. With the characterization of the microbiome and of its functional properties inferred through predictive metagenomics, a series of proteins were identified as biomarkers in the water phase that could be correlated directly to corrosion. This study provides an opportunity for the further development of a protein-based biomarker approach for effective and reliable microbial corrosion detection and monitoring in the field.

Introduction

Microbiologically influenced corrosion (MIC) can be involved in the deterioration of steel and other structural materials in a wide range of industries, and its economic impacts may be highly significant (Bennett, 1978). In particular, within the oxygen-free engineered environments of oil and gas operations, MIC often becomes the dominant process. Microbes responsible for MIC in production pipelines of the petroleum industry are typically affiliated to many different Bacteria and Archaea, organized in microbial communities with different levels of interactions. The composition of such pipelines' microbiome will ultimately govern the occurrence of specific microbial metabolisms, and thus the extent of microbial corrosion. Specifically for pipelines, the local conditions can vary quickly. For example, temperatures closer to the wellhead are usually several degrees higher than in the center of the pipeline and, especially for offshore deep pipelines, seasonal temperature variability can be observed even for buried pipelines (Sund et al., 2015). Similarly, pH can vary dramatically in relation to mixing with water from various sources and because of abiotic and biotic generation of H_2S (Hutcheon, 1998) and CO_2 (Bai et al., 2018). Shear stress deriving from pipeline flow can also hinder especially planktonic microbes (Rochex et al., 2008). To partially alleviate these drawbacks, microbial communities inside pipelines tend to attach to the inner wall, preferentially at the bottom, or "6 o'clock position," where the water and oil phases separate and where the flow velocity and shear stress are lower (Nakayama, 2018). Additionally, the 6 o'clock position in pipelines, can accumulate particles, especially in the presence of bends (Leung et al., 2018), providing a potential source of macronutrients, such as N and P, as well as micronutrients, such as Cu, Fe, Mn, and S. In the presence of a surface for

attachment, water and nutrients, the pipeline's microbiome can establish by forming a biofilm, which is likely to be a prerequisite for the occurrence of MIC (Eckert, 2015). The central role of sulfate-reducing bacteria (SRB) as main culprit of MIC has been extensively reported (Beech et al., 1994; Booth, 1964; Hamilton, 1985; Lee et al., 1995; Paisse et al., 2013). SRB in pure cultures can cause corrosion via organotrophic or lithotrophic growth (Enning & Garrelfs, 2014). In the first case, an organic substrate is normally used as electron donor for sulfate reduction (Muyzer & Stams, 2008), while in the second scenario, the iron from steel serves directly as electron donor (Enning et al., 2012). Under both organotrophic and lithotrophic conditions, hydrogen, generated either biologically or abiotically, might also constitute a suitable electron donor for SRB. Under every electron donor regime, moreover, release of H_2S as main byproduct of sulfate reduction facilitates the corrosion of steel (Wikjord et al., 1980). Furthermore, other microbial electron-accepting metabolisms, with either organic carbon, H_2 or Fe from steel as electron donor, have been described as responsible for MIC. These include nitrate-reduction (Hubert et al., 2005), thiosulfate-reduction (Magot et al., 1997), methanogenesis (Mori et al., 2010), and acetogenesis (Dowling et al., 1992; Mand et al., 2014). Even though a vast amount of knowledge on MIC exists, an effective and economic approach to detect and monitor MIC is still lacking (Little et al., 2020). Here, we hypothesize that a diverse soil microbiome can guarantee the establishment of corrosive microbial consortia under different, including nonmesophilic, conditions. In this study, we enriched anaerobically a natural microbial community from marine soil under various physiochemical conditions and in the presence of carbon steel. These conditions were chosen to mimic several parameters, such as variability in temperature, pH, and CO_2 concentrations, often detected in oil and gas production pipelines. Microbiologically mediated changes in

water chemistry (e.g., sulfate and acetate) were recorded and interpreted in light of the observed corrosion rates and changes in the microbial community composition. Additionally, we applied predictive metagenomics to elucidate the potential metabolic processes occurring in the enrichments. Our results reveal a strong correlation between culturing conditions, such as temperature, CO_2 concentration, pH, presence of organic substrates, and corrosion. MIC was higher under mesophilic conditions, and never observed at 60°C. Furthermore, although sulfate was present in every condition tested, sulfate reduction was observed only in limited amount, and it was not correlated with corrosion rates. The original marine microbial community shifted to a more specialized consortium, with several members of the Desulfovibrionales and Clostridiales accounting for more than 60% of the total microbiome's composition in samples with higher corrosion rates. Although the order Desulfovibrionales were present in most of the samples, different species of the genus *Desulfovibrio* were actually enriched under the various conditions tested. Finally, predictive metagenomics showed higher potential for genes related to chemotaxis; biofilm formation; and for various transporters of amino acids, peptides, and iron. Taken all together, our results indicate that there might be a limit for MIC under nonmesophilic conditions and that, although SRB were often present in samples where MIC occurred, their presence alone, or the incidence of sulfate reduction, was not always indicative of MIC. The latter is particularly relevant for MIC monitoring and diagnostics, since SRB signatures or sulfate reduction tests are often used for onsite MIC assessment, while more specific biomarkers able to unambiguously detect biological corrosion might be more desirable.

Materials and Methods
Sample Collections and Setup of Lab Enrichments

Coastal marine sediment was collected in sterile glass bottles on the northeastern tip of Galveston Island, Texas. The silt, gray-black sediment was taken from approximately 3 to 15 cm depth and smelled of hydrogen sulfide. The collection bottle was filled up to minimize oxygen exposure, and then sent to the lab under cooling. The original sediment microbial community reported in Table S1 was analyzed using amplicon pyrosequencing with the Titanium chemistry on an FLX Genome Sequencer (Roche 454 Life Sciences, Branford, CT, USA). Liquid culturing medium was prepared by adding the following components (all from Sigma-Aldrich, St. Louis, MO, USA) to MilliQ water: KH_2PO_4 (0.5 g/l), NH_4Cl (1 g/l), $CaCl_2$ (0.41 g/l), NaCl (15.5 g/l), KCl (0.11 g/l), and $MgCl_2$ (0.33 g/l); 20 mM (2.84 g/l) Na_2SO_4 was also added as electron acceptor. Afterward, the liquid phase of the medium was purged with N_2 for 35 min and 2-(N-morpholino) ethanesulfonic acid (MES) added as buffer (6.5 g/l), as well as resazurin (0.2 mg/l) as oxygen indicator. Also, 80 μl/l of 70% thioglycolic acid and 1.25 g/l L-cysteine were included as reducing agents. Subsequently, the liquid was further purged with CO_2:N_2 (either at 15:85 or 7:93, vol/vol) for 15 min, and the bottle was equipped with butyl stoppers and O-ring screw caps, through which ~180 ml of headspace gases were removed prior to autoclaving at 120°C for 40 min. After autoclaving and cooling the medium, 1 ml of the following solutions, prepared as described (Aeckersberg et al., 1991), were added anaerobically: trace metals, vitamin mixture, thiamine, riboflavin, vitamin B12, selenite-tungstate, phosphate, and ammonium. Finally, 180 ml of either 7% or 15% CO_2 was added to the headspace of the medium and the pH was eventually adjusted to the final values with 1 M of either HCl or NaOH.

Then, 80 ml of medium was dispensed in 120-ml serum bottles equipped with butyl stoppers and crimped with aluminum rings. Also the liquid phase and the headspace of each serum bottle were flushed with 15% CO_2 for about 5 min each. Initial inoculum of approximately 1.5 g of sediment slurry was enriched and 2 ml of such enrichment were repeatedly transferred to fresh medium bottles until virtually sediment-free cultures were obtained. From the latter, 2 ml were then transferred to fresh serum bottles for each given condition. These final bottles were equipped with a unique tailor-made coupon holder consisting of a Teflon threaded rod and bolts holding in place 2 Teflon discs with slots for fitting two X-52 carbon steel coupons (5 × 20 × 1 mm) per holder. Each cleaned steel coupon, with a 600-grit sandpaper surface finish, was weighted in triplicate prior to serum bottle assembling. Each holder hung suspended from the neck of a serum bottle via a thin nylon wire piercing the butyl stopper of the bottle (Fig. S1). Assembled bottles and holders were flushed with oxygen-free nitrogen through a heated, H_2-reduced, copper furnace (Supelco), and then autoclaved prior to medium addition.

Half of the bottles contained acetate (10 mM) and propionate (5 mM) as organic carbon source and electron donor, while the other half did not contain any organic carbon and both were set at different initial, buffer-controlled pH (5, 6.5, and 8). The entire series of conditions was replicated for CO_2 concentrations of either 7 or 15% in N_2. Furthermore, an extra series of bottles containing organic carbon source, 15% CO_2 but no inoculum was set as negative controls. All the bottles were incubated at selected temperatures (20, 40, and 60°C) and under moderate shaking (60 rpm) for approximately 2 months.

Time-Resolved Monitoring of Anions from Enrichments' Water Phase

Duplicate anion quantification using high-pressure ion chromatography (HP-IC) was applied on 1 ml of subsamples collected at least weekly. An HP-IC 5000 + Reagent-Free system (Thermo-Fisher Scientific, Massachusetts, USA) equipped with Dionex Ion-Pac AS 11-HC column, EluGen® III Potassium Hydroxide capillary cartridge and suppressed conductivity detector Dionex ACES 300, was used for the analyses. All the samples were centrifuged at 5,000 rpm for 2.5 min and the supernatants were filtered through 0.2-µm cellulose acetate filters to remove the particulate and biological matter and then diluted 1:100 for final analysis. The pump flow rate was 1 ml/min; injection volume of the samples was 25 μl and a column temperature of 30°C was used. An eluent gradient method was established for separation of acetate, propionate, and sulfate. The KOH gradient started with initial concentration of 1 mM for 1 min and then at increments of 0.3 mM/min from 1 to 12 min, 5 mM for 13 min, 20 mM for 25 min, and final 20 mM hold for 35 min. Calibration standards with known concentrations of acetate, propionate, and sulfate were prepared as well and used to quantify the samples.

Corrosion Product Analysis and Quantification of Corrosion Rates

Biofilms on the coupon surface were removed by vortexing (2,500 rpm, 5 min) and sonication (40 kHz, 15 min) and the resulting biomass from both the planktonic and biofilm phase was collected by centrifugation (3,500 rpm, 30 min, and 4°C). The resulting supernatants were discarded and the pellets were immediately frozen at –80°C for molecular analyses. The coupon with remaining biomass and corrosion products were further vortexed at maximum speed for additional 5 min in acetone. Subsequently,

the acetone phase was filtered using Anodisc filter membrane (47 mm in diameter with a pore size of 0.02 μm) and the corrosion products were collected and analyzed by a Rigaku Mini-Flex II X-ray diffraction (XRD) system for phase identification. The coupons, now free of biofilm and loose corrosion products, were examined with a LEO Gemini 1530 scanning electron microscope (SEM), along with energy dispersive X-ray spectroscopy (EDS) for surface residual corrosion product analysis. Coupons with corrosion product or scale left on the surface after biofilm removal were also analyzed by XRD to identify the crystal structure of the corrosion products. After the corrosion products were analyzed, the scale was removed from each coupon using a passive Clarke solution (20 g Sb_2O_3 and 50 g $SnCl_2$ dissolved in 1 L of 36% HCl, (G1–03, 2011)) and the weight of the descaled coupon was recorded. General weight loss dependent corrosion rate of each coupon was determined by measuring the difference between pre- and posttest coupon weights, as described in ASTM G1-03 standard (G1–03, 2011). Triplicate weights of descaled metal coupons were recorded to calculate corrosion rates in mm/year, using the formula:

$$kw/(At\rho)$$

where k is a constant ($k = 8.76 \times 10^4$), w is the weight loss (initial—final weight) in grams, A is the surface area of the metal coupons in cm^2 ($1\ cm^2$), t is the incubation time in hours ($\sim$1,440 hr), and ρ is the density of the material in g/cm^3 ($7.85\ g/cm^3$ for X-52 carbon steel). Factor analysis on covariance from corrosion data of the enrichments (excluding negative controls) was performed using the maximum likelihood method with varimax rotation as implemented in SAS JMP® Pro V 15.1.0.

DNA Extraction, Next-Generation Sequencing and Bioinformatics

Pellets from one of the two biological replicates were suspended in 2 ml of phosphate buffered saline (PBS, pH 7.4) and DNA was extracted using the E.Z.N.A.® Soil DNA Kit, following the manufacturer protocol except for the skipped column-purification step. Extracted total DNA was sequenced using MetaVx™ 16S rDNA next-generation sequencing library preparations and Illumina MiSeq sequencing at GENEWIZ, Inc. (South Plainfield, NJ, USA). Briefly, the DNA was used to generate amplicons that cover V3, V4, and V5 hypervariable regions of bacteria and archaea 16S rDNA. Indexed adapters were added to the ends of the 16S rDNA amplicons by limited cycle PCR. Sequencing libraries were validated using a DNA chip for the Agilent 2100 Bioanalyzer (Agilent Technologies, Palo Alto, CA, USA), and quantified by Qubit and real-time PCR (Applied Biosystems, Carlsbad, CA, USA). DNA libraries were multiplexed and loaded on an Illumina MiSeq instrument according to manufacturer's instructions (Illumina, San Diego, CA, USA). Base calling were conducted by the MiSeq Control Software (MCS) on the MiSeq instrument. Raw data were analyzed using QIIME2 as described (Bolyen et al., 2019). Briefly, raw forward and reverse paired-end reads were trimmed for quality and the Illumina adaptors were removed using Dada2 (Callahan et al., 2016), as implemented in QIIME2. Subsequently, denoised data were clustered and classified to assign the appropriate taxonomy for every operational taxonomic unit (OTU). For certain OTUs of interest, that is, those affiliated with Deltaproteobacteria and Clostridia, manual classification using NCBI's nucleotide Basic Local Alignment Search Tool (https://blast.ncbi.nlm.nih.gov) was performed. OTU counts and sequences of each OTU were also used for predictive metagenomics using Picrust2 (Douglas et al., 2020), with the standard pipeline as described (https://github.com/picrust/picrust2/wiki/Full-pipeline-script). Predictive metagenomics output tables,

as KEGG orthologs (https://www.genome.jp/kegg/) for each sample were also normalized and used for further analysis, using the Python library Pandas (https://pandas.pydata.org/). DNA sequences have been submitted to NCBI's Short Reads Archive and are available under the Bioproject PRJNA658599, with accession numbers from SAMN15879593 to SAMN15879609.

Results
Time-Resolved Monitoring of Anions from Enrichments' Water Phase

Fig. 1 shows the ion chromatography (IC) measurement results of sulfate from all the enrichment. Complete removal of the starting sulfate concentration of 20 mM was observed only in MIC enrichments at 20°C and pH 6.5 when organic carbon was present. More than 50% of the starting sulfate concentration was reduced under the same conditions lithotrophically. Of the other enrichments at 20°C, the organotrophic culture at pH 8 and 7% CO_2, was also removing more than 50% of the sulfate, while no more than 5 mM were reduced for any condition at pH 5. At 40°C and pH 6.5, most of the enrichments reduced $\sim$50% of the sulfate, except for the lithotrophic culture with 7% CO_2. For the other enrichments at 40°C, at pH 5 the sulfate reduced was $\sim$8 mM, except for the organotrophic enrichment with 7% CO_2 and, at pH8, only the organotrophic enrichment at 15% CO_2 removed $\sim$50% of the sulfate. Little or no sulfate respiration was otherwise observed for all the other treatments as well as for the negative controls. Similarly, acetate mineralization was achieved only by microbes at 20°C and pH 6.5. Additionally, we observed acetate production in various enrichments at both 20 and 40°C under different pH (Fig. S2). At 20°C and pH 6.5, an initial acetate production that almost doubled its original concentration to $\sim$20 mM, was followed by consumption to $\sim$1.7 mM. Contrariwise, at 40°C, acetate values of $\sim$25 and $\sim$20 mM were measured at pH 5 and 6.5, respectively, until the end of the experiment. Interestingly, acetate was detected up to $\sim$15 mM also in lithotrophic enrichments at 20 and 40°C, even though there was no acetate in the solution at the beginning of the experiments (Fig. S3). Propionate was consumed only in few of the organotrophic enrichments, especially at 40°C (Fig. S2). Similarly to the sulfate profiles, no changes in acetate or propionate were detected at 60°C and in all the negative controls (Fig. S2).

Corrosion Rate and Corrosion Product Analysis

Corrosion rates calculated from weight loss are reported in Fig. 2. A temperature gradient, with decreasing corrosion from lower to higher temperatures, can be observed for all the treatments at pH 6.5. In general, enrichments at pH 6.5 produced thick black biofilms and higher corrosion rates. In the presence of organic carbon at pH 6.5, minimal differences in corrosion rates were observed between 20 and 40°C, as well as for different CO_2 concentrations. On the other hand, for lithotrophic enrichments at pH 6.5, corrosion rates were reduced more than 35% at 40°C compared to 20°C. Corrosion rates measured at pH 5 where significantly lower than those at pH 6.5, and a generally higher background corrosion was present, due to the acidic pH. Nevertheless, several enrichments at 20 and 40°C showed visible biofilms and produced moderate corrosion rates, compared to the corresponding controls. Finally, very low corrosion rates as well as biofilm formation, barely distinguishable from the abiotic controls, were observed at pH 8. For all the conditions, 60°C apparently constituted the upper limit for microbial growth of corrosive microbes. Opposite trend of corrosion rates with increasing temperatures
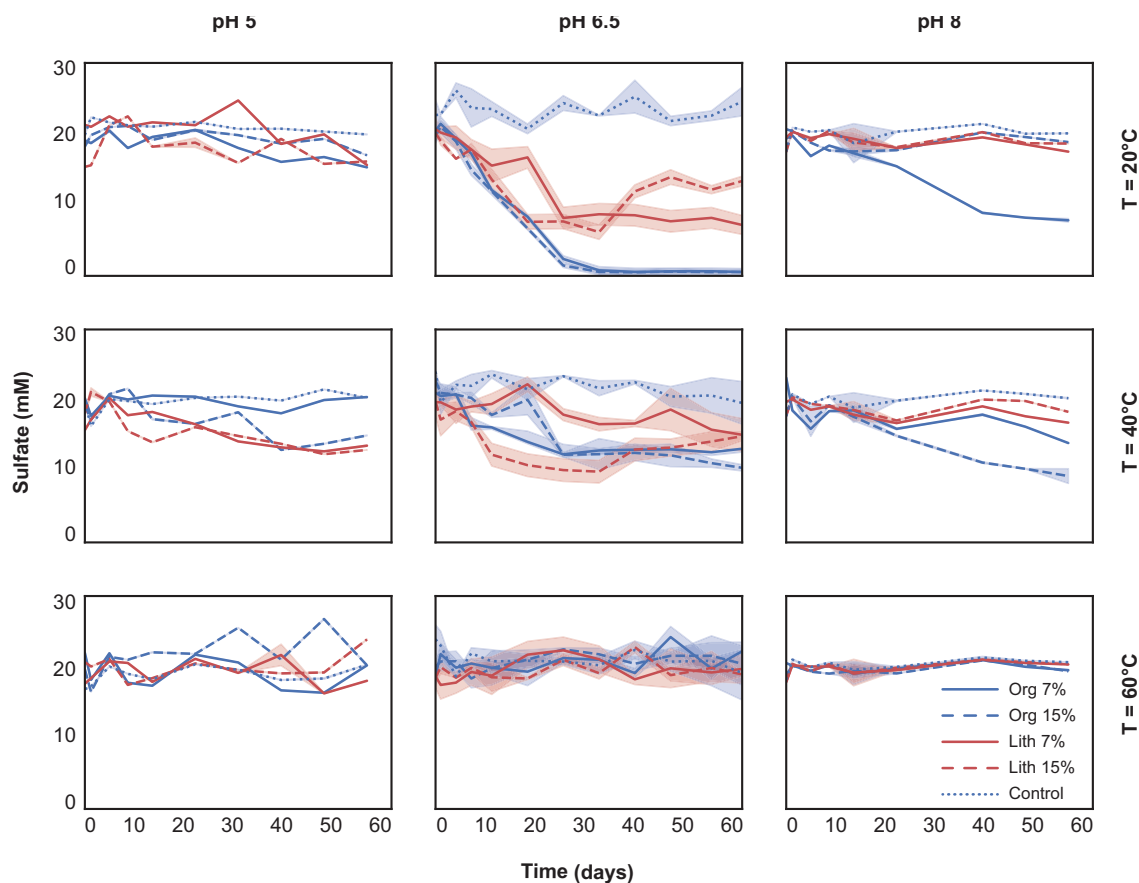
Fig. 1. Ion chromatography (IC) measurements of sulfate from enrichments growing either organotrophically (Org, blue) or lithotrophically (Lith, red). Negative control (dotted line) was prepared as organotrophic, but contained no inoculum. Shaded areas represent standard deviation from duplicate IC measurements.
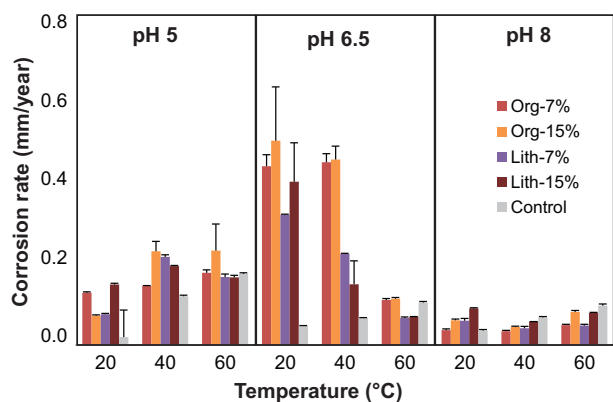

Fig. 2. Corrosion rates calculated from weight loss measurement of duplicate coupons. Samples are grouped by temperature (x axis), pH (boxes), growth condition (organotrophic, orange and lithotrophic, purple) and CO_2 concentration (different shades).

was observed for negative control samples as compared to biological samples, with higher corrosion rate at higher temperature. At the end of the test, black corrosion products were observed in both the liquid phase and on the coupon surface for all the treatments, except for tests at 60°C and sterile controls. Statistical analysis of corrosion rates in relation to the different physical–chemical conditions revealed a strong correlation between corrosion rates and pH especially in the organotrophic

enrichments, whereas the lithotrophic enrichments did not exhibit any particular correlation (Fig. S4). XRD and SEM/EDS analyses indicated no corrosion product formation on coupons tested at 60°C and sterile controls. For both organotrophic and lithotrophic enrichments at 20 and 40°C, XRD analysis of the entrained solids within the biofilm and the corrosion scale or residual solids adhered to the coupon surface after biofilm removal detected mackinawite (FeS) as the primary corrosion product, besides halite (NaCl), vivianite (Fe$_3$(PO$_4$)$_2$ ·8(H$_2$O)), and occasionally trace amounts of siderite (FeCO$_3$) at pH 6.5 only. This is consistent with the SEM/EDS analysis of the coupon surfaces where mackinawite was identified as the predominant corrosion product, as shown in Fig. S4. Additionally, small amount of greigite (Fe$_3$S$_4$) was also detected by XRD, along with mackinawite, for the tests at pH 5 and 20°C (data not shown).

Characterization of Microbial Communities

Selected samples, based on the IC and corrosion rate profile, were subjected to 16S rDNA amplicon sequencing, as shown in Fig. 3. More than 98% of the microbial community, consisting of 1,204 unique OTU, belonged to the Bacteria domain, while Archaea were scarcely represented. Consistently with the observed corrosion data, DNA was hardly extractable from samples growing at 60°C and from most of the samples at pH 8, due to the low biomass present in these samples. The original marine beach soil revealed a mixed microbial community characterized especially by Bacteroidetes, Cyanobacteria, Desulfobacterales, and
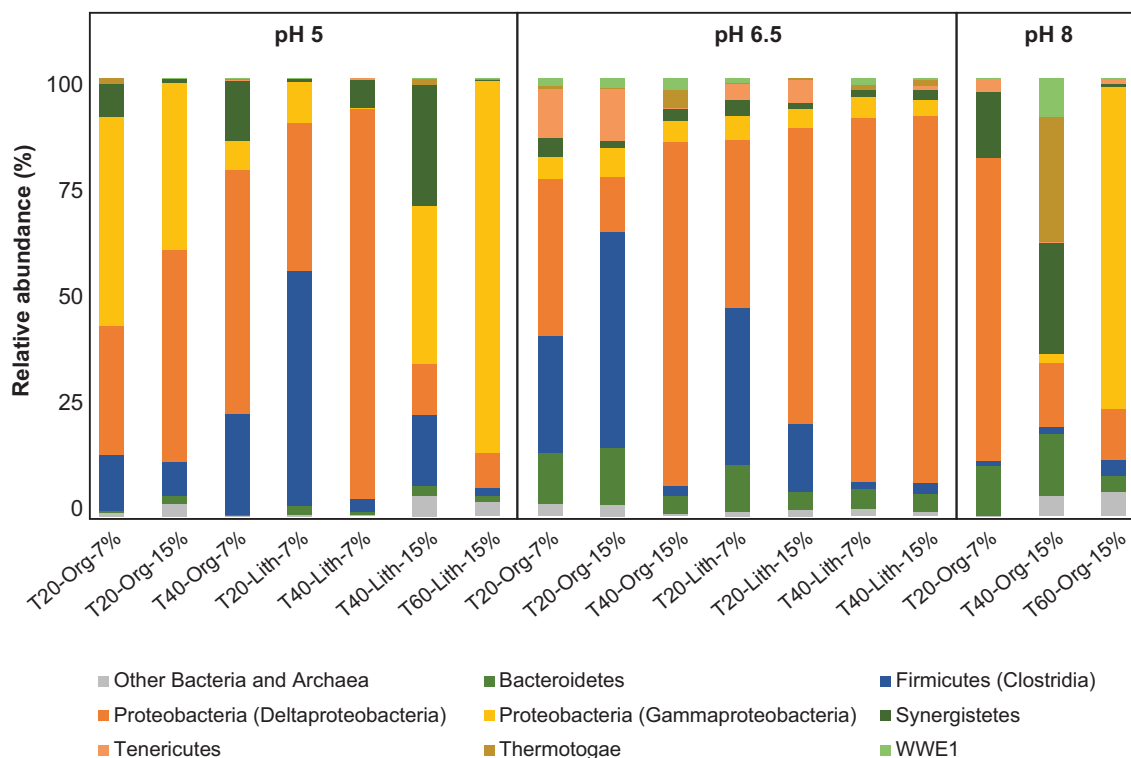
Fig. 3. Microbial community characterization of selected samples from corrosion enrichments. Classification is shown at a Phylum/Class level. Names on the x-axis summarize the condition as T (temperature, 20, 40, or 60°C), metabolism (organotrophic or lithotrophic), and CO_2 concentration (7 or 15%). Boxes group samples by pH.

unclassified strains of Gammaproteobacteria, along with a high number of unclassified lineages (Table S1). On the other hand, enriched consortia were represented by only 7 phyla, accounting for more than 95% of the overall diversity: Bacteroidetes, Firmicutes, Proteobacteria, Synergistetes, Tenericutes, Thermotogae, and WWE1. Additionally, Firmicutes were almost exclusively Clostridia, while Gammaproteobacteria and Deltaproteobacteria were the main representatives of Proteobacteria (Fig. 3). Given the higher relative abundance of Deltaproteobacteria and Clostridia, and their relevance in MIC studies, a breakdown of these two Classes, based on BLAST of the specific OTUs belonging from those Classes (Tables S2 and S3), is shown in Fig. 4. In terms of Deltaproteobacteria, most of the samples from pH 6.5, characterized by higher corrosion rates (above 0.2 and up to 0.5 mm/year), shared higher relative abundance of *Desulfovibrio salexigens* (Fig. 4A). This microbe was the single most abundant OTU in our dataset, accounting for more than 16% of all the reads sequenced. Additionally, other deltaproteobacterial SRB enriched at pH 6.5 included *Desulfobacter hydrogenophilus*, particularly relevant at 20°C under organotrophic conditions, *Pseudodesulfovibrio indicus*, enriched especially under lithotrophic conditions, and *Desulfocurvus thunnarius*, significant mostly at 40°C. The main outlier from the enrichments at pH 6.5 was represented by the enrichment of *Desulfovibrio pshycrotolerans*, up to 15% in relative abundance only in the lithotrophic sample growing at 40°C with 15% CO_2. This sample was characterized by a steep decrease in sulfate at the beginning of the experiment and partial sulfate production toward the end, and the corrosion rate was also substantially lower (0.15 mm/year). The deltaproteobacterial population differed profoundly in the enrichments at pH 5, with only three main lineages, *Desulfovibrio tunisiensis*, *Desulfovibrio dechloracetivorans,* and *Desulfobacter hydrogenophilus*,

enriched with poor correlation with corrosion data. Similarly, at pH 8, *D. dechloracetivorans* and *D. thunnarius* were the main members of the community, with the addition of *Desulfosarcina variabilis* enriched at 40°C only. Clostridia distribution reflects somehow what observed for Deltaproteobacteria, with increased diversity at pH 6.5 compared to pH 5 and very low abundance at pH 8 (Fig. 4B). An additional peculiarity of the enrichments at pH 6.5 was that, unlike Deltaproteobacteria, Clostridia were strongly limited by temperature, with low relative abundance at 40°C and by electron donor, with organotrophic enrichments presenting counts more than double of those from the lithotrophic ones. The main lineages enriched at pH 6.5 were related to *Aminipila butyrica*, *Dethiosulfatibacter aminovorans*, *Soehngenia saccharolytica*, *Clostridium tepidum,* and *Clostridiisalibacter paucivorans*. At pH 5, no real correlation with temperature or electron donor was present and, similarly to what observed with Deltaproteobacteria, a different and less diverse community was observed, with microbes affiliated to *Lacrimispora amygdalina*, *Hungateiclostridium clariflavum*, *Serpentinicella alkaliphila,* and *Fusibacter tunisiensis*.

Another important bacterial group enriched especially at pH 5, was characterized by a strong presence of the gammaproteobactrial genus *Pseudomonas* (Fig. 3) and by moderate corrosion rates (above 0.13 mm/year). These samples also contained smaller relative abundances of *Serratia marcenses* within the Gammaproteobacteria subdivision. Intriguingly, the other two samples presenting higher abundance of Gammaproteobacteria, that is, the organotrophic enrichments growing at pH 5, 20°C and 15% CO_2 and at pH 8, 60°C and 15% CO_2, both with low corrosion rates (below 0.08 mm/year), were characterized by a different gammaproteobacterial population, with members of the genus *Halomonas* dominating the community along with lower abundances of the genus *Shewanella* (data not shown). Among the
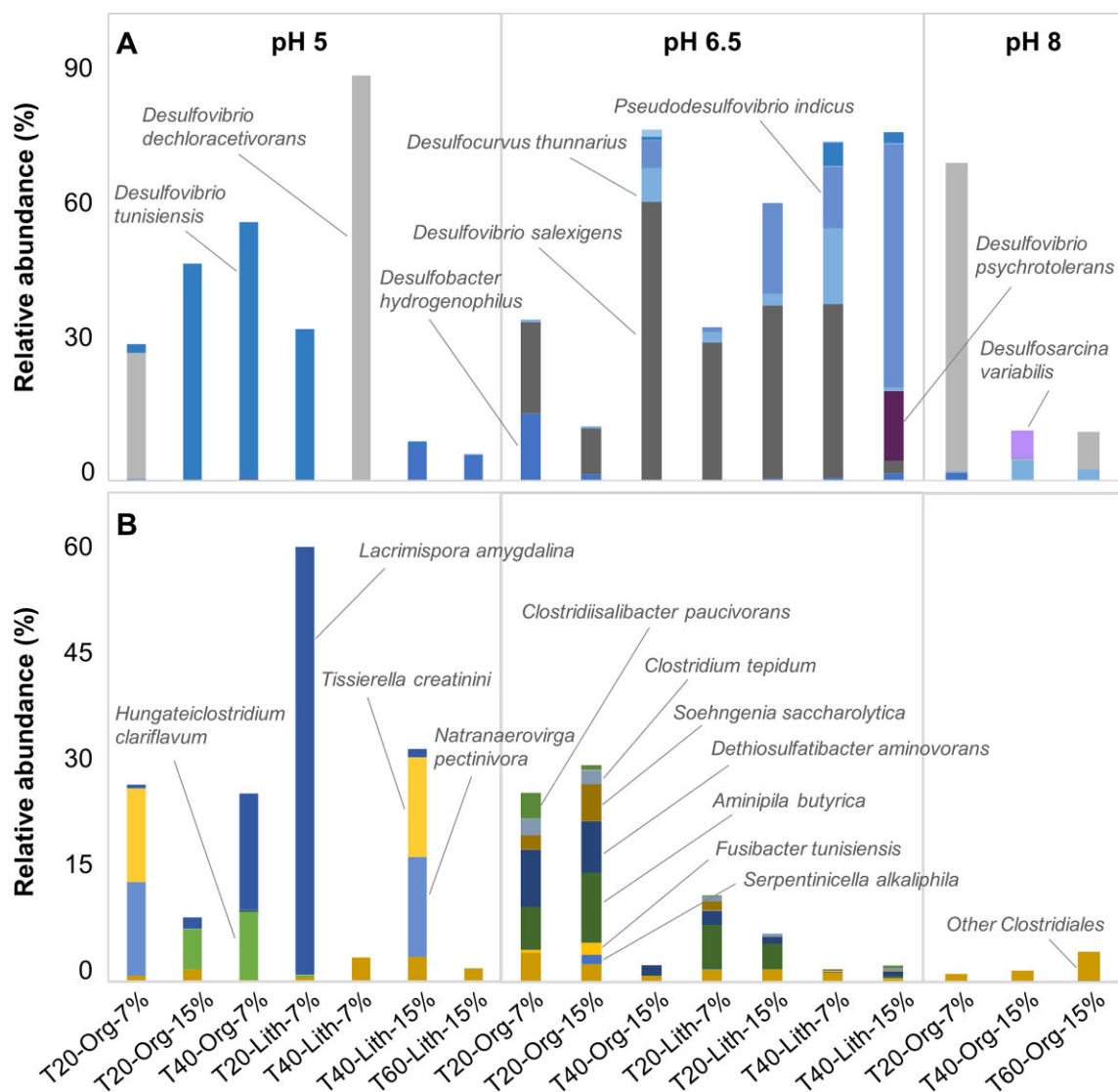
Fig. 4. Breakdown of the most representative microbial lineages, Deltaproteobacteria (A) and Clostridiales (B) in all the enrichments. Naming and grouping as in Fig. 3.

other phyla detected, the Dethiosulfovibrionaceae family within Synergistetes was enriched, up to 25%, especially at pH 8, similarly to Thermotogae and WWE1, also present mainly at pH 8. Bacteroidetes were also present in most of the samples, up to 14% in relative abundance and were largely affiliated to the Rikenellaceae family.

Predictive Metagenomics

A total of 6,522 predicted genes from the overall experiment microbiome were obtained after removal of singletons. The average Nearest Sequenced Taxon Index (NSTI) was 0.104 ± 0.015, pointing to a reasonable predictions for the metagenomes of our samples, especially considering that this mixed microbial community likely contained 16S rDNA sequences for which sequenced genomes are not readily available (Douglas et al., 2020). In order to verify that the predictions were consistent with the 16S rDNA profiling, we confirmed that genes central to sulfate reduction were representatives of the proportions of sulfate reducers present in our samples. As reported in Fig. S6, the relative abundance of the KEGG orthologs K00394 and K00395 (adenylylsulfate reductase subunits A and B, respectively) as well as K11180 and K11181 (dissimilatory

sulfite reductase alpha and beta subunits, respectively) were predicted with highly similar profiles ($R^2 = 98.3\%$) to that reported for the 16S rDNA analyses of the Deltaproteobacteria (Fig. 4A) which were, in fact, largely sulfate-reducing bacteria. Among all the other predicted genes relevant across the entire dataset (Table S4), several were associated to protein responsible for chemotaxis, through the two-component system, and for transport across the membrane. Within the transport proteins, ABC transporters, polar and branched amino acid transporters, and ferrous iron uptake systems were the ones with highest relative abundance across several enrichments (Table S4). Pearson correlation coefficients calculated for the predictive metagenome against corrosion rates are shown in Table S5. The relative abundances of the four KEGG orthologs with the highest Pearson coefficients are plotted against the corrosion rates in Fig. 5 and are discussed in more detail.

Discussion

The physical and chemical testing conditions of the experimental setup did have a significant impact on MIC. Our original hypothesis was that a natural microbial community from sediment could
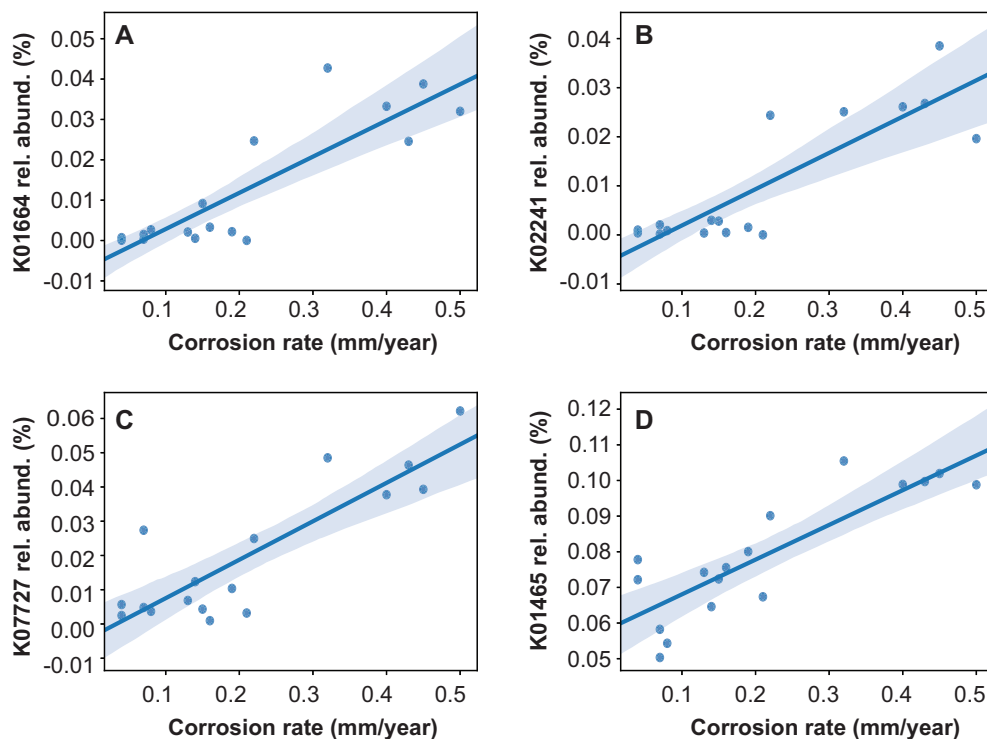
Fig. 5. Correlation between selected proteins from predictive metagenomics and corrosion rates. The proteins are expressed as relative abundance of the normalized functional profiling predicted with Picrust2 and are named using the corresponding KEGG ortholog ID. Shaded areas represent 95% confidence interval.

harbor enough diversity to grant microbial corrosion under a large variety of physiochemical parameters. Our experiments only partially validated the hypothesis, since MIC was not detectable at higher temperature and alkaline pH. Although the role of MIC at temperatures of ~50°C has been previously reported (Alfaro-Cuevas-Villanueva et al., 2006; Lata et al., 2012), and even if the limit of microbial life is well above 60°C, MIC occurrence at higher temperatures remains unclear. Mardhiah and colleagues reported corrosion by pure cultures of *Desulfovibrio vulgaris* at temperatures as high as 60°C (Mardhiah et al., 2014). However, the limited amount of corrosion observed (up to 0.06 mm/year) suggests a passivation phenomenon rather than active biocorrosion. A more environmental-oriented study from Comanescu et al. found that water injection pipelines for secondary oil recovery with average temperatures 50–60°C presented deeper pits and higher bacterial counts than those with average temperatures between 60 and 120°C (Comanescu et al., 2012). Although interesting, such study is probably less relevant for production pipelines, since a low amount of oxygen is present in water injection pipelines, along with different pools of electron donors and acceptors, correlated with the origin of the waters (groundwater, seawater, or river/lakes). Recently, studies from Li and colleagues from the Jiangsu oilfield (Yangzhou, Jiangsu, China) reported molecular analyses from several oil wells (Li et al., 2016, 2017), showing potential for corrosion up to ~0.2 mm/year at fairly high reservoir temperatures (66–80°C). Evaluation of corrosion, however, was performed by immersion of the steel coupons in glass bottles filled with waters from the well. Since dissolved H_2S from souring in these water-flooded wells was present, the primary cause of corrosion could have been abiotic rather than biologically induced. In our study, on the other hand, high corrosion, up to ~0.5 mm/year, can be detected at moderate temperatures of 20 and 40°C, but MIC was always dubious at 60°C and, if it

occurred, it was never to any large extent. SRB dominated the community under some of the most corrosive conditions. The most represented SRB at pH 6.5, *Desulfovibrio salexigens*, is a marine microbe that requires more than 0.5% NaCl for growth, which is consistent with the NaCl concentration of our medium (1.5%). Species related to *D. salexigens* isolated, along with other Desulfovibrionaceae, from corroded steel samples in coastal South Vietnam (Tarasov & Borzenkov, 2015), were able to utilize hydrogen, but not acetate. The conditions presenting some of the higher relative abundance of *D. salexigens* in our study were also correlated to higher corrosion rates, sulfate reduction, and concomitant presence of Clostridia, especially for the enrichments at 20°C. Several Clostridiales are able to consume acetate, producing CO_2 and H_2, to fuel a well-known cometabolism in which SRB can outcompete methanogens to remove the hydrogen (Lovley et al., 1982). At the same time, many microbes, including SRB, can also ferment amino acids, producing even more acetate (Barker, 1981). These observations are well in line with the acetate production measured in our experiment (Figs. S2 and S3), as well as with the high amount of amino acid transport proteins computed as predicted metagenome (Table S4). In the presence of an active SRB community, biogenic H_2S reacting with the steel could also produce H_2 while forming FeS (mackinawite). The predominance of mackinawite, suggesting metabolic activity of SRB and an SRB-induced corrosion mechanism in our test system, is corroborated by XRD and SEM/EDS analyses (Fig. S5) and is consistent with previous studies (Hamilton, 1985; McNeil & Little, 1990). At temperatures of 40°C, however, Clostridiales were strongly reduced but partial sulfate reduction, acetogenesis, and moderate to high corrosion were still observed. Under this scenario, amino acid fermentation would still produce acetate but, since the clostridial partner converting acetate to H_2 and CO_2 is strongly reduced in relative abundance, accumulation of acetate is observed (Fig. S2). As a

consequence of diminished H_2, also sulfate reduction is hampered in these enrichments (Fig. 1), similarly to what shown for different environments (Nanninga & Gottschal, 1985). Additional observations from our predictive metagenomics analyses (Table S4) also indicated a high potential for proteins involved in iron transport and regulation systems (K02013-K02016, K03711, and K04758). Although these proteins are mainly related to siderophores and assimilatory iron metabolisms, the role of iron regulation or chelation in microbes correlated to MIC remains unclear.

The conditions found at pH 5 were to some extent similar to those described for pH 6.5, with the caveat that different SRB and clostridial subpopulations were enriched. Of particular note, *Desulfovibrio dechloracetivorans* was isolated for its ability to grow oxidizing acetate and reducing 2-chlorophenol, but can also use sulfate as electron acceptor (Sun et al., 2000). Despite such metabolism is available to *D. dechloracetivorans*, the extent of sulfate reduction is limited to some of the enrichments growing at 40°C, both organotrophically and lithotrophically. In both cases, furthermore, acetate is produced, pointing to a similar fermentative metabolism of that observed at pH 6.5.

As above mentioned, some members of Gammaproteobacteria were also detected in our study, especially at pH 8. Although not correlated to the most corrosive conditions in our study, *Serratia marcenses* has been previously reported in corrosion studies (Rajasekar et al., 2011) and species of *Shewanella* and *Halomonas* are well known for their role in the iron cycle (Sanchez-Porro et al., 2010; Shi et al., 2007).

Some of the conditions examined in our study might represent a good approximation of the temperature and pH in pipelines subjected to MIC. Yet, most of the popular methods for assessment of MIC, such as sulfate tests or 16S rDNA detection of SRB, would not inform about the difference in corrosion. In fact, only when coupons were analyzed for corrosion rates, the true extent of MIC could be evaluated in our enrichments. However, coupons tests are not always available in the field, especially for offshore pipelines in remote location and, therefore, there is a need for biomarkers that unambiguously correlate liquid-phase samples to MIC. Our samples were collected including both planktonic and biofilm phases, since large flocks of biofilms were detaching from the coupons and sonication/vortexing of the coupons was used, adding more biofilm material to the bulk planktonic phase. This approach can be approximated to a lab-scale simulation of the removal of biofilm caused by pipelines' flow and subsequent collection of the water fraction from a transport pipeline. Although we did not perform functional genomics or transcriptomics, we employed predictive metagenomics to explore the possibility for hypothesis testing on the microbiome functions using the cheap and widely available 16S rDNA amplicon sequencing. Our results show several genes coding for proteins potentially correlated to corrosion (Table S5). As examples, in Fig. 5 we reported four of these proteins exhibiting the highest Pearson correlation coefficients in relation to corrosion. The pabA protein, responsible for the synthesis of para-aminobenzoate (KEGG orthology K01664, Fig. 5A), has been shown to stimulate growth of members of the genus *Desulfovibrio* isolated from sewage digestors (Ueki & Suto, 1981). The competence protein comFB (K02241, Fig. 5B) has unknown, probably regulatory function in DNA uptake (Sysoeva et al., 2015), which is a process also possibly related to surface attachment (Bakkali, 2013). The putative Cro/CI transcriptional regulator (K07727, Fig. 5C) is a protein that modulates the lytic cycle in bacteriophages; the beneficial role of bacteriophage lysis in biofilm formation has been described (Gödeke et al., 2011) and in our lab we also found its relevance for *D. vulgaris* biofilms (Pilloni

et al., 2018). Finally, the pyrC protein is a dihydroorotase involved in uracil monophosphate (UMP) biosynthesis (K01465, Fig. 5D), which is a quorum sensing and biofilm regulator well studied especially in microbes like *Pseudomonas aeruginosa* (Ueda et al., 2009). The advantage of using these biomarkers over more classical 16S rDNA or SRB-specific genes is that the metabolic products of the specific proteins could be measured via simple biochemical methods instead of using costly and time-consuming molecular methods. For example, pabA could be detected colorimetrically using existing tests (Bratton et al., 1939). Similarly, measurement of UMP through enzymatic conversion to UDP and detection of ATP-induced luminescence is possible (Yoshida et al., 2012). Such protein-based approach would mean a fast, reliable, and economically feasible method for MIC control programs in the field.

Conclusions

This study shows that dramatic changes happened to a natural mixed microbial community when shifting to a corrosive consortium. Physical and chemical conditions caused further rearrangements, with consequent differences in the extent of corrosion. Our work provides evidences of potential interactions, based on acetate cycling, between SRB and Clostridia during MIC in oil production environments and identifies proteins potentially correlated to corrosion. Our results can be further tested to develop better tools for the monitoring and mitigation of microbial corrosion *in situ*.

Supplementary Material

Supplementary material is available online at *JIMB* (*www.academic.oup.com/jimb*).

Acknowledgments

Conflict of Interest

The authors declare no conflict of interest.

References

Aeckersberg, F., Bak, F., & Widdel, F. (1991). Anaerobic oxidation of saturated-hydrocarbons to CO_2 by a new type of sulfate-reducing bacterium. *Archives of Microbiology*, 156(1), 5–14.

Alfaro-Cuevas-Villanueva, R., Cortes-Martinez, R., García-Díaz, J. J., Galvan-Martinez, R., & Torres-Sanchez, R. (2006). Microbiologically influenced corrosion of steels by thermophilic and mesophilic bacteria. *Materials and Corrosion*, 57(7), 543–548.

Bai, H., Wang, Y., Ma, Y., Zhang, Q., & Zhang, N. (2018). Effect of CO_2 partial pressure on the corrosion behavior of J55 carbon steel in 30% crude oil/brine mixture. *Materials (Basel, Switzerland)*, 11(9), 1765.

Bakkali, M. (2013). Could DNA uptake be a side effect of bacterial adhesion and twitching motility? *Archives of Microbiology*, 195(4), 279–289.

Barker, H. A. (1981). Amino acid degradation by anaerobic bacteria. *Annual Review of Biochemistry*, 50(1), 23–40.

Beech, I. B., Cheung, C. W. S., Chan, C. S. P., Hill, M. A., Franco, R., & Lino, A. R. (1994). Study of parameters implicated in the biodeterioration of mild-steel in the presence of different species of sulfate-reducing bacteria. *International Biodeterioration & Biodegradation*, 34(3-4), 289–303.

Bennett, L. H. (1978). *Economic effects of metallic corrosion in the United States: A report to the congress*: U.S. Department of Commerce, National Bureau of Standards.

Bolyen, E., Rideout, J. R., Dillon, M. R., Bokulich, N. A., Abnet, C. C., Al-Ghalith, G. A., Alexander, H., Alm, E. J., Arumugam, M., Asnicar, F., Bai, Y., Bisanz, J. E., Bittinger, K., Brejnrod, A., Brislawn, C. J., Brown, C. T., Callahan, B. J., Caraballo-Rodríguez, A. M., Chase, J., … Caporaso, J. G. (2019). Reproducible, interactive, scalable and extensible microbiome data science using QIIME 2. *Nature Biotechnology*, 37(8), 852–857.

Booth, G. H. (1964). Sulphur bacteria in relation to corrosion. *Journal of Applied Bacteriology*, 27(1), 174–181.

Bratton, A. C., Marshall, E. K., Babbitt, W. t. t. a. o. D., & Hendrickson, A. R. (1939). A new coupling component for sulfanilamide determination. *Journal of Biological Chemistry*, 128(2), 537–550.

Callahan, B. J., McMurdie, P. J., Rosen, M. J., Han, A. W., Johnson, A. J. A., & Holmes, S. P. (2016). DADA2: High-resolution sample inference from Illumina amplicon data. *Nature Methods*, 13(7), 581–583.

Comanescu, I., Taxen, C., & Melchers, R. E. (2012). *Assessment of MIC in carbon steel water injection pipelines*. Society of Petroleum Engineers, SPE 155199.

Douglas, G. M., Maffei, V. J., Zaneveld, J., Yurgel, S. N., Brown, J. R., Taylor, C. M., Huttenhower, C., & Langille, M. G. I. (2020). PICRUSt2: An improved and customizable approach for metagenome inference. *bioRxiv*, 672295.

Dowling, N. J. E., Brooks, S. A., Phelps, T. J., & White, D. C. (1992). Effects of selection and fate of substrates supplied to anaerobic-bacteria involved in the corrosion of pipe-line steel. *Journal of Industrial Microbiology*, 10(3-4), 207–215.

Eckert, R. B. (2015). Emphasis on biofilms can improve mitigation of microbiologically influenced corrosion in oil and gas industry. *Corrosion Engineering, Science and Technology*, 50(3), 163–168.

Enning, D. & Garrelfs, J. (2014). Corrosion of iron by sulfate-reducing bacteria: new views of an old problem. *Applied and Environmental Microbiology*, 80(4), 1226–1236.

Enning, D., Venzlaff, H., Garrelfs, J., Dinh, H. T., Meyer, V., Mayrhofer, K., Hassel, A. W., Stratmann, M., & Widdel, F. (2012). Marine sulfate-reducing bacteria cause serious corrosion of iron under electroconductive biogenic mineral crust. *Environmental Microbiology*, 14(7), 1772–1787.

G1-03 ASTM. (2011). *Standard practice for preparing, cleaning, and evaluating corrosion test specimens*. ASTM International.

Gödeke, J., Paul, K., Lassak, J., & Thormann, K. M. (2011). Phage-induced lysis enhances biofilm formation in Shewanella oneidensis MR-1. *The ISME journal*, 5(4), 613–626.

Hamilton, W. A. (1985). Sulfate-reducing bacteria and anaerobic corrosion. *Annual Review of Microbiology*, 39,1, 195–217.

Hubert, C., Nemati, M., Jenneman, G., & Voordouw, G. (2005). Corrosion risk associated with microbial souring control using nitrate or nitrite. *Applied Microbiology and Biotechnology*, 68(2), 272–282.

Hutcheon, I. (1998). The potential role of pyrite oxidation in corrosion and reservoir souring. *Journal of Canadian Petroleum Technology*, 37(01), 5.

Lata, S., Sharma, C., & Singh, A. (2012). Microbial influenced corrosion by thermophilic bacteria. *Central European Journal of Engineering*, 2(1), 113–122.

Lee, W., Lewandowski, Z., Nielsen, P. H., & Hamilton, W. A. (1995). Role of sulfate-reducing bacteria in corrosion of mild-steel - a review. *Biofouling*, 8(3), 165–194.

Leung, T., Been, J., Beauregard, Y., & Chow, J. (2018). *Modelling particle sedimentation in oil pipelines*. Paper presented at the CORROSION 2018, Phoenix, Arizona, USA.

Li, X.-X., Liu, J.-F., Yao, F., Wu, W.-L., Yang, S.-Z., Mbadinga, S. M., Gu, J.-D., & Mu, B.-Z. (2016). Dominance of Desulfotignum in sulfate-reducing community in high sulfate production-water of high temperature and corrosive petroleum reservoirs. *International Biodeterioration & Biodegradation*, 114, 45–56.

Li, X.-X., Liu, J.-F., Zhou, L., Mbadinga, S. M., Yang, S.-Z., Gu, J.-D., & Mu, B.-Z. (2017). Diversity and composition of sulfate-reducing microbial communities based on genomic DNA and RNA transcription in production water of high temperature and corrosive oil reservoir. *Frontiers in Microbiology*, 8(1011).

Little, B. J., Blackwood, D. J., Hinks, J., Lauro, F. M., Marsili, E., Okamoto, A., Rice, S. A., Wade, S. A., & Flemming, H. C. (2020). Microbially influenced corrosion—Any progress? *Corrosion Science*, 170, 108641.

Lovley, D. R., Dwyer, D. F., & Klug, M. J. (1982). Kinetic analysis of competition between sulfate reducers and methanogens for hydrogen in sediments. *Applied and Environmental Microbiology*, 43(6), 1373–1379.

Magot, M., Ravot, G., Campaignolle, X., Ollivier, B., Patel, B. K. C., Fardeau, M. L., Thomas, P., Crolet, J. L., & Garcia, J. L. (1997). Dethiosulfovibrio peptidovorans gen. nov, sp. nov, a new anaerobic, slightly halophilic, thiosulfate-reducing bacterium from corroding offshore oil wells. *International Journal of Systematic Bacteriology*, 47(3), 818–824.

Mand, J., Park, H. S., Jack, T. R., & Voordouw, G. (2014). The role of acetogens in microbial influenced corrosion of steel. *Frontiers in Microbiology*, 5, 1–14.

Mardhiah, I., Noor, N. M., Nordin, Y., Arman, A., Rosilawati, M. R., & Ahmad, S. A. R. (2014). Effect of pH and temperature on corrosion of steel subject to sulphate-reducing bacteria. *Journal of Environmental Science and Technology*, 7(4), 209–217.

McNeil, M. B. & Little, B. J. (1990). Technical note: Mackinawite formation during microbial corrosion. *Corrosion*, 46(7), 599–600.

Mori, K., Tsurumaru, H., & Harayama, S. (2010). Iron corrosion activity of anaerobic hydrogen-consuming microorganisms isolated from oil facilities. *Journal of Bioscience and Bioengineering*, 110(4), 426–430.

Muyzer, G. & Stams, A. J. M. (2008). The ecology and biotechnology of sulphate-reducing bacteria. *Nature Reviews Microbiology*, 6(6), 441–454.

Nakayama, Y. (2018). Chapter 6 - Flow of viscous fluid. In Y. Nakayama (Ed.), *Introduction to fluid mechanics* (2nd ed., pp. 99–133). Butterworth-Heinemann.

Nanninga, H. J. & Gottschal, J. C. (1985). Amino acid fermentation and hydrogen transfer in mixed cultures. *FEMS Microbiology Letters*, 31(5), 261–269.

Paisse, S., Ghiglione, J. F., Marty, F., Abbas, B., Gueune, H., Amaya, J. M. S., Muyzer, G., & Quillet, L. (2013). Sulfate-reducing bacteria inhabiting natural corrosion deposits from marine steel structures. *Applied Microbiology and Biotechnology*, 97(16), 7493–7504.

Pilloni, G., Chatterjee, M., & He, K. (2018). Methods to assess monitor and control bacterial biofilms. US Patent Application, 0051309(A1).

Rajasekar, A., Balasubramanian, R., & Vm Kuma, J. (2011). Role of hydrocarbon degrading bacteria *Serratia marcescens* ACE2 and *Bacillus cereus* ACE4 on corrosion of carbon steel API 5LX. *Industrial & Engineering Chemistry Research*, 50(17), 10041–10046.

Rochex, A., Godon, J.-J., Bernet, N., & Escudié, R. (2008). Role of shear stress on composition, diversity and dynamics of biofilm bacterial communities. *Water Research*, 42(20), 4915–4922.

Sanchez-Porro, C., Kaur, B., Mann, H., & Ventosa, A. (2010). Halomonas titanicae sp. nov., a halophilic bacterium isolated from the RMS Titanic. *International Journal of Systematic and Evolutionary Microbiology*, 60(Pt 12), 2768–2774.

Shi, L., Squier, T. C., Zachara, J. M., & Fredrickson, J. K. (2007). Respiration of metal (hydr)oxides by Shewanella and Geobacter: A key role for multihaem c-type cytochromes. *Molecular Microbiology*, 65(1), 12–20.

Sun, B., Cole, J. R., Sanford, R. A., & Tiedje, J. M. (2000). Isolation and characterization of Desulfovibrio dechloracetivorans sp. nov., a marine dechlorinating bacterium growing by coupling the oxidation of acetate to the reductive dechlorination of 2-chlorophenol. *Applied and environmental microbiology*, 66(6), 2408–2413.

Sund, F., Oosterkamp, A., & Hope, S. M. (2015). *Pipeline modeling – Impact of ambient temperature and heat transfer modeling. Paper presented at the the Twenty-fifth International Ocean and Polar Engineering Conference*, Kona, Hawaii, USA.

Sysoeva, T. A., Bane, L. B., Xiao, D. Y., Bose, B., Chilton, S. S., Gaudet, R., & Burton, B. M. (2015). Structural characterization of the late competence protein ComFB from Bacillus subtilis. *Bioscience Reports*, 35(2).

Tarasov, A. L. & Borzenkov, I. A. (2015). Sulfate-reducing bacteria of the genus Desulfovibrio from South Vietnam seacoast. *Microbiology (Reading, England)*, 84(4), 553–560.

Ueda, A., Attila, C., Whiteley, M., & Wood, T. K. (2009). Uracil influences quorum sensing and biofilm formation in Pseudomonas aeruginosa and fluorouracil is an antagonist. *Microbial biotechnology*, 2(1), 62–74.

Ueki, A. & Suto, T. (1981). Vitamin requirement of sulfate-reducers isolated from sewage digestor fluids. *The Journal of General and Applied Microbiology*, 27(3), 229–237.

Wikjord, A. G., Rummery, T. E., Doern, F. E., & Owen, D. G. (1980). Corrosion and deposition during the exposure of carbon-steel to hydrogen sulfide-water solutions. *Corrosion Science*, 20(5), 651–671.

Yoshida, T., Nasu, H., Namba, E., Ubukata, O., & Yamashita, M. (2012). Discovery of a compound which acts as a bacterial UMP kinase PyrH inhibitor. *FEMS Microbiology Letters*, 330(2), 121–126.